

# Complexity of Spider Dragline Silk

Ali D. Malay, Hamish C. Craig, Jianming Chen, Nur Alia Oktaviani, and Keiji Numata\*



Cite This: *Biomacromolecules* 2022, 23, 1827–1840



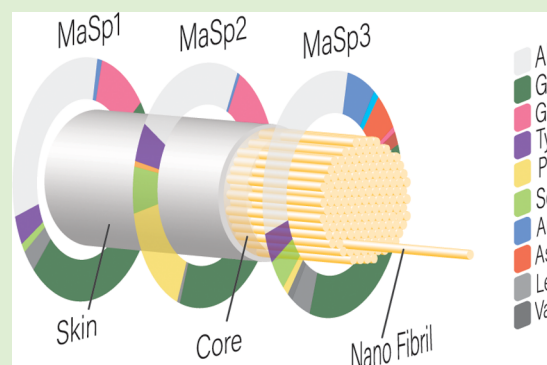
Read Online

ACCESS |

Metrics & More

Article Recommendations

**ABSTRACT:** The tiny spider makes dragline silk fibers with unbeatable toughness, all under the most innocuous conditions. Scientists have persistently tried to emulate its natural silk spinning process using recombinant proteins with a view toward creating a new wave of smart materials, yet most efforts have fallen short of attaining the native fiber's excellent mechanical properties. One reason for these shortcomings may be that artificial spider silk systems tend to be overly simplified and may not sufficiently take into account the true complexity of the underlying protein sequences and of the multidimensional aspects of the natural self-assembly process that give rise to the hierarchically structured fibers. Here, we discuss recent findings regarding the material constituents of spider dragline silk, including novel spidroin subtypes, nonspidroin proteins, and possible involvement of post-translational modifications, which together suggest a complexity that transcends the two-component MaSp1/MaSp2 system. We subsequently consider insights into the spidroin domain functions, structures, and overall mechanisms for the rapid transition from disordered soluble protein into a highly organized fiber, including the possibility of viewing spider silk self-assembly through a framework relevant to biomolecular condensates. Finally, we consider the concept of "biomimetics" as it applies to artificial spider silk production with a focus on key practical aspects of design and evaluation that may hopefully inform efforts to more closely reproduce the remarkable structure and function of the native silk fiber using artificial methods.



## 1. INTRODUCTION

From antiquity to the present era, spiders' ability to spin beautiful and functional silken structures, unmatched in nature, has evoked a deep fascination in mankind.<sup>1</sup> From the standpoint of science, too, spider silk has inspired generations of researchers, mainly for the remarkable properties of the fiber, whose mechanical performance and hierarchical organization are still unmatched by the most sophisticated artificial materials.

This Perspective is not intended to be a comprehensive review of the topic of spider silks, excellent examples of which are thankfully available.<sup>2–5</sup> Rather, we wish to take this opportunity to highlight some recent developments in the field and then consider what these could mean in terms of future research directions. The discussion is focused mainly on dragline (major ampullate) silk, which is by far the most studied type of spider silk. The first part will explore the complexity of spider dragline silk in terms of its physical constituents. In recent years, reports from the next-generation sequencing front have begun to hint at a more nuanced picture of dragline silk composition than previously anticipated, findings that might require a reassessment of the conventional and relatively simple two-component model based on MaSp1 and MaSp2. Next, we turn to the functions of the individual spidroin domains and discuss the different frameworks that can

be used to understand and further explore the silk self-assembly mechanisms with an emphasis on more recent findings. We subsequently tackle the topic of *biomimetics*, where we ask the question what constitutes a true biomimetic approach for making spider silk? We highlight several studies that have claimed to apply biomimetic principles in making artificial spider silks and provide suggestions for possible future directions.

## 2. COMPLEX COMPOSITION OF SPIDER DRAGLINE SILK

**Spidroins: Beyond MaSp1 and MaSp2.** It is well established that spider dragline silk fiber (a.k.a. major ampullate silk) is assembled from structural proteins called spidroins, which come in two main subtypes, MaSp1 and MaSp2. The two subtypes have similar overall sequence architectures, which can be described as a highly repetitive core region that is flanked by small N-terminal and C-terminal

Received: December 25, 2021

Revised: March 14, 2022

Published: April 4, 2022



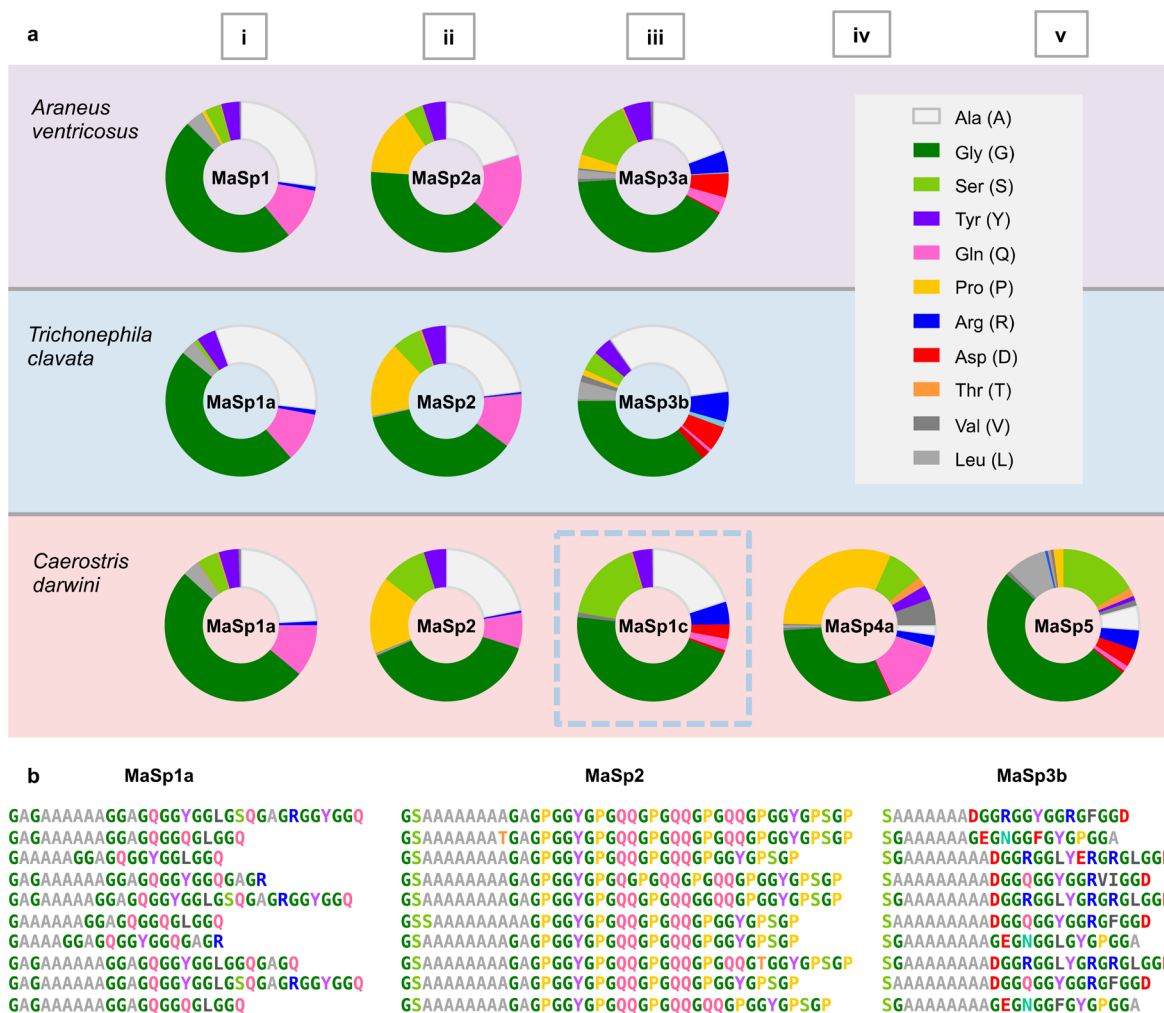


**Figure 1.** Analysis of the amino acid sequences of the dragline silk spidroins from 3 orbweaver species. (a) Residue abundance of the MaSp repetitive regions from *A. ventricosus*,<sup>19</sup> *T. clavata*,<sup>18</sup> and *C. darwini*.<sup>17</sup> Residue types are color coded according to the legend on the right. Sequence designations are indicated in the middle of the circles and follow the nomenclature used in the respective studies. Vertical columns denote (i) MaSp1, (ii) MaSp2, (iii) MaSp3-like, (iv) MaSp4, and (v) MaSp5 sequences. Interestingly, a sequence denoted as MaSp1c from *C. darwini* bears a close resemblance to MaSp3 from the other 2 species (dotted-line box). (b) Consecutive tandem repeats from the full-length sequences of MaSp1a, MaSp2, and MaSp3b from *T. clavata*.<sup>18</sup>

domains (NTD and CTD, respectively). The repetitive regions, which make up ~90% of the primary structure, consist of alternating runs of polyalanine and multiple glycine-rich motifs arrayed in tandem (in the form mostly of GX and GGX, with X representing a limited selection of residues). Across the spider taxa, the main difference between MaSp1 and MaSp2 sequences lies in the motif composition of the repetitive domains, with MaSp1 showing a relatively high incidence of Q, A, and L occupying the X position in (G)GX motifs in the glycine-rich regions, whereas an abundance of proline (usually in the context of GPG) and diglutamine motifs (QQ) tends to be diagnostic for MaSp2.<sup>6–8</sup> It has been theorized that the appearance of MaSp2 during evolution has enabled spider dragline silks to exploit a far wider tensile property space (mostly in terms of greater extensibility and hence toughness) compared to fibers composed of MaSp1 alone.<sup>9</sup> The relative abundance of MaSp1 and MaSp2 in dragline fiber seems to vary by species as well as according to factors like nutrition.<sup>10–12</sup>

Interestingly, a number of recent studies, spurred mostly by advances in proteomics and sequencing technologies, paint a

more complex picture of dragline silk composition than is provided by a simple MaSp1/MaSp2 dichotomy.<sup>13–20</sup> A subtype termed MaSp3 was identified in several species via proteomics and genomic target capture techniques.<sup>15,16</sup> On the other hand, a major study by Babb et al. reported at least 8 distinct subtypes of spidroins in the major ampullate silk of *Trichonephila clavipes* (denoted as MaSp-a to MaSp-h, plus other putative spidroins).<sup>14</sup> From the Darwin's bark spider (*Caerostris darwini*), Garb et al. obtained a MaSp4 sequence whose repeat regions are notable for the absence of poly-Ala runs and an abundance of Pro, Gln, and Val residues as well as MaSp5, whose repetitive sequences are mostly composed of GGX motifs.<sup>17</sup> The presence of MaSp4 has been linked to the extreme toughness of *C. darwini* dragline.<sup>17,20,21</sup> Kono et al. used a combination of genomic, transcriptomic, and proteomic approaches to identify spidroin sequences from *Araneus ventricosus*,<sup>19</sup> which identified the MaSp3 subtype (later assigned to MaSp3A) as the third main component after MaSp1 and MaSp2. The same group likewise identified three main components in the dragline silk from the Nephilinae lineage: MaSp1, MaSp2, and MaSp3B,<sup>18</sup> with the latter being

apparently synonymous with the previously identified Sp-74867 spidroin from *T. clavipes*.<sup>14</sup> Curiously, despite highly similar repetitive sequences, an analysis of the terminal domain sequences suggests that the MaSp3 sequence from *A. ventricosus* (MaSp3A) and from the nephilid taxa (MaSp3B/C) is descended from different spidroin lineages,<sup>18,19</sup> suggesting the possibility of convergent evolution. It is also worth noting here that the nomenclature surrounding the newer, alternative MaSp and spidroin variants still has not stabilized in the literature, perhaps owing, at least partly, to the fragmentary nature of sequence data assembly inherent in the methods and to the rapid pace of publication of large sequence data sets. Apart from finding an expanded array of MaSp sequences, recent studies have also shown evidence for cross-expression of spidroins among silk types, as exemplified by AcSp1 spidroin (normally associated with prey-wrapping silk) in dragline fiber.<sup>15,22</sup>

Figure 1a illustrates the amino acid compositions of the repetitive regions from the different MaSp subtypes of *A. ventricosus*, *T. clavata*, and *C. darwini*, which represent three main lineages within the diverse orb-weaver family Araneidae.<sup>23</sup> As is well known, MaSp repetitive sequences employ a limited palette of amino acids, dominated by only a few residue types. We show that the sequences can be arranged according to residue composition (columns) with a high degree of conservation across the species. The compositions of MaSp1 (column i) and MaSp2 (column ii) are well known and have been discussed elsewhere.<sup>8</sup> Focusing on the MaSp3-like sequences (column iii), we see an abundance of Gly and Ala residues in the repetitive regions that is comparable to MaSp1/2; however, what is different is the appearance of charged residues, particularly Asp (acidic) and Arg (basic), that are found in nearly equal measure, and which is accompanied by a concomitant decrease in the proportion of Gln residues, relative to the MaSp1 and MaSp2 sequences. We also point out that this MaSp3 pattern matches well with one of the sequences identified in *C. darwini* (which the authors designated as MaSp1c), supporting the conservation of this subtype across species. MaSp4 (column iv) and MaSp5 (column v) have so far only been identified in bark spiders.<sup>17,20</sup> Figure 1b shows the typical arrangement of the amino acid motifs in the repetitive regions of the three main MaSp subtypes (in this case, from *T. clavata*).<sup>18</sup>

In dragline silk fiber, the relative abundance of the different spidroin components is thought to exert an important influence on the mechanical properties of the corresponding fibers, as seen, for instance, with analysis of MaSp1/MaSp2 levels.<sup>9,11,12,24</sup> The presence of the newly described MaSp subtypes within dragline silk would thus also be expected to have an effect on the mechanical performance, especially if these variants are present in substantial levels. In this regard, proteomics experiments have found a relatively high abundance of such variants in dragline fiber, estimated at 11–16% in the case of MaSp4 in *C. darwini*, while MaSp3A was found to be actually the most abundant subtype in *A. ventricosus*. Although initial work using short versions of recombinant MaSp1, MaSp2, and MaSp3 based on sequences from *T. clavata* did not reveal obvious correlations between the sequences and the behavior,<sup>18</sup> a more focused experimental approach designed to probe specific questions would likely yield important insights.

It is also emphasized that so far very little is known about the interactions among different MaSp subtypes in the native fiber,

including between MaSp1 and MaSp2. It is conceivable that differences in the chemical properties of the repetitive regions would lead to a nonrandom distribution of MaSp subtypes in the silk dope that might facilitate the apparently nonrandom distribution of spidroin subtypes within the dragline fiber, as some have reported.<sup>25,26</sup>

In addition to these questions, we also propose that there is more to be gained from a more careful study of the MaSp repetitive sequences. Typically, these are understood simply in terms of the crystal-forming or “hard” poly-Ala regions versus the more amorphous or “soft” Gly-rich regions. However, apart from the treatment of Pro (found in MaSp2) in terms of its unique effects on peptide backbone conformations<sup>27</sup> and its involvement in supercontraction,<sup>28</sup> there have been relatively few insights on the roles of the other conserved residues on the structure and function of dragline silk (as an exception, a recent study found a possible link between Tyr residues and supercontraction<sup>29</sup>). Yet, there is clearly sequence conservation across the different spider taxa,<sup>8</sup> suggesting that the composition and arrangement of residues within the glycine-rich regions have some biological relevance. Why, for instance, do we consistently find an abundance of Gln (Q) in MaSp1/MaSp2 but not Asn (N) despite having presumably very similar chemical properties? Why are the different residue types patterned in particular ways but not others (for instance, a Tyr-Tyr motif is never seen)? One possibility is that the repetitive sequences are optimized for solubility and/or phase transitions during silk self-assembly, and indeed, there are intriguing parallels between the sequence of the MaSp repetitive domains and certain intrinsically disordered proteins that are associated with liquid–liquid phase separation (see below).

**Nonspidroin Components.** It is often overlooked that aside from the structural spidroins, native spider silk has a diverse complement of molecular constituents that include glycoproteins, other nonspidroin proteins, lipids, and pigments, etc., often heterogeneously distributed along the skin–core architecture of the fiber cross-section.<sup>26,30–34</sup>

Here, we focus briefly on recent findings regarding nonspidroin protein constituents of spider dragline silk. Much of the pioneering work was done on silk from the cobweb spinning black widow (*Latrodectus sp.*; Theridiidae), where transcriptomic and proteomic analyses have yielded a diverse profile of silk-associated proteins.<sup>15,22,35–37</sup> Interestingly, a novel array of cysteine-rich proteins (CRPs) was found to be expressed in the fiber with yet unclear biological function. Various unclassified proteins were also identified as well as putative variants of cysteine-rich secretory protein (CRISP3) and fasciclin.<sup>22</sup>

Arakawa and co-workers published a series of studies aimed at elucidating the protein constituents of silks from members of the orb-weaving spider family Araneidae, including *A. ventricosus*,<sup>19</sup> the Nephilinae subfamily,<sup>18</sup> and bark spiders (*Caerostris spp.*).<sup>20</sup> Several nonspidroin proteins with relatively low molecular weights have been detected in appreciable quantities in the dragline silk, to which the term SpiCE (for spider silk constituting element) has been collectively applied. Interestingly, a considerable subset of the SpiCE sequences also harbors a high abundance of cysteine residues, consistent with a CRP designation. Also intriguing is that there appears to be rather low sequence conservation among the SpiCE variants, even for closely related species.<sup>18,19</sup>

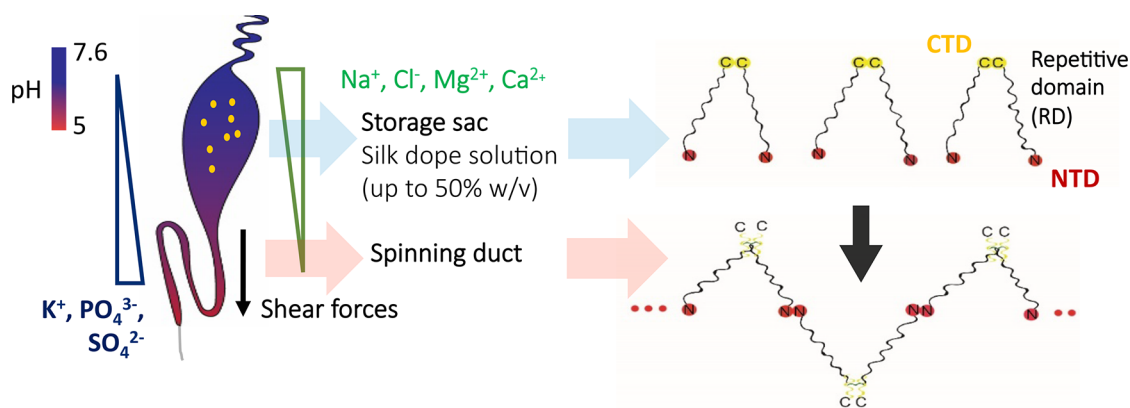


**Figure 2.** Schematic representations of the spider major ampullate silk gland (left) and of MaSp spidroin polypeptide chains (right). Precursor spidroins can maintain a soluble state for prolonged periods in the gland sac as a concentrated liquid feedstock (silk dope) despite adopting largely intrinsically disordered conformations. During the fiber formation process, the spidroins travel down the s-shaped spinning duct, where they enter a multidimensional state of flux. Changes encountered in the duct include a pH gradient (neutral to acidic), ion exchange (shift from chaotropic to kosmotropic ions), dehydration, and elongational and shear forces (imparted by the progressively narrowing duct geometry); together these produce rapid and precisely timed structural transitions in the individual spidroin domains (NTD, RDD, CTD) that somehow lead to the formation of macroscopic silk fibers having a characteristic hierarchical organization.

To probe a possible structural role, materials made from composite blends of recombinant dragline spidroin and SpiCE-NMa1 (the most common SpiCE variant with an estimated abundance of 1% in the dragline fiber based on proteomics studies) were tested for changes in mechanical properties. The results show that SpiCE-NMa1 contributed to an increased tensile strength in the case of composite silk films, even at low concentrations; in contrast, however, it imparted a negative effect on the tensile strength of the composite silk fibers.<sup>18</sup> As it stands, the biological function of nonspidroin proteins in dragline silk is still a largely unexplored topic. Apart from acting as structural elements, roles in communication, protection, or prey capture may be envisioned; supporting the latter view, for instance, CRPs feature prominently as constituents of biological toxins.<sup>38</sup>

**Post-Translational Modification.** Another aspect of structural complexity that is largely ignored is post-translational modification (PTM), which generally entails the enzymatic modification of certain amino acids after protein biosynthesis. PTMs play an essential role in the correct folding and function of many proteins. A foremost example in structural proteins is proline hydroxylation in collagen; without this PTM the procollagen strands cannot achieve their characteristic triple-helix structure.<sup>39</sup> Within spider silk, little is known about the exact role and structural impact of PTMs;<sup>40</sup> however, both MaSp1 and MaSp2 have been shown to carry phosphorylated serine and tyrosine residues within the repetitive region.<sup>41,42</sup> The position and enhancement of negative charge associated with the phosphorylation has known impacts on formation of helical structures in other proteins and show similar patterns in spider silk with a molecular model of MaSp1 incorporating phosphorylate serine and tyrosine showing increased coil formation with greater formation of alpha helices and a reduction of the amount of 3<sub>10</sub> helices than in previous models.<sup>43</sup>

The presence of the oxidized residue dityrosine has also been confirmed within MaSp1 and MaSp2;<sup>41,42</sup> however, little is yet known about its exact abundance or structural role within spider silk. Dityrosine is known to also form in small amounts within Tussah silk, forming cross-links in the crystalline region.<sup>44</sup> Although in this case dityrosine is not

thought to have any impact on the physicochemical properties of the silk, the utility of dityrosine cross-linkage however will likely prove to be an important tool in de novo development of future biomaterials.<sup>45</sup>

A hydroxylated form of tyrosine and an intermediate in the formation of dityrosine 3,4-dihydroxyphenylalanine (DOPA) has also been shown to be present in marine silk from caddisfly larvae and sandcastle worms. It is utilized as an adhesive sight used to bind dissimilar materials under aqueous conditions.<sup>46–48</sup> A further example of PTMs being necessary for adhesion within silk can be observed in the gumfoot threads found in *Latrodectus*. The glycosylation of residues within the MA silk appears to play an important role in the adhesive properties of gumfoot glue to the lines that form the capture threads within these species.<sup>49</sup> This highlights the potential of PTMs not just for the production of manmade silks but also for structurally intrinsic functionalization of silk with other properties such as adhesion.

The most recent PTM to be identified in spider silk is hydroxyproline, which has been demonstrated in both major ampullate and flagelliform silks.<sup>50,51</sup> The hydrogen-bonding site added to proline through hydroxylation in the constituent MaSp2 and Flag repetitive regions is thought to add to the mechanoelastic properties of these fibers. This demonstrates the importance of detailed proteomic understanding of silk, pivotal when modeling the silk structure necessary for a holistic understanding of silk's structure–function relationship.

Ultimately our understanding of the silk proteome is still in its infancy when compared to our current genomic, transcriptomic, and structural knowledge. The influence PTMs have on protein assembly and the resultant protein structure may prove to be a pivotal factor in understanding the structure–function relationship within spider silk. Moreover, it may be an important consideration in the production and functionalization of biomimetic silks with comparable material prosperities to those of natural spider silk.<sup>45</sup>

### 3. STRUCTURE AND FUNCTION OF INDIVIDUAL DOMAINS

Inside the ampullate gland, the spidroins are in a highly solubilized state (liquid feedstock) despite its high concen-

tration (up to 50% w/v).<sup>52</sup> The spidroins are transformed into insoluble fiber through the combined effects of pH and ion gradients as well as extensional and shear forces as they migrate down the spinning ducts<sup>53,54</sup> (Figure 2). The pH in the gland storage sac was found to be slightly basic (pH 7.6) and progressively gets more acidic down the spinning duct toward the spinnerets.<sup>53</sup> Ion exchange is believed to occur, with chaotropic ions ( $\text{Na}^+$ ,  $\text{Cl}^-$ ,  $\text{Mg}^{2+}$ ) predominating in the sac, while along the spinning duct, the concentration of kosmotropic ions ( $\text{PO}_4^{3-}$ ,  $\text{SO}_4^{2-}$ ) was found to increase.<sup>54</sup>

The changes in pH and ion compositions in the spider gland are strongly related to the changes in the structures and properties of dragline silk during the spinning process. Using native and recombinant spider dragline proteins, various studies have investigated the spinning mechanism of spider silk formation.<sup>53,55–57</sup> Spidroins have modular sequence architectures, and each domain is thought to play distinct and essential roles during silk fiber formation. Despite the small relative size of the terminal domains, both NTD and CTD are essential for orchestrating precise fiber assembly under native conditions<sup>58,59</sup> and are found to be well conserved through evolution.<sup>60,61</sup>

The NTD exists in monomeric form at pH 7 in the presence of 300 mM NaCl,<sup>62,63</sup> while more acidic (pH 5.5) and lower NaCl conditions, which resemble the conditions in the spinning duct, promote the dimerization of NTD with an antiparallel orientation.<sup>64</sup> Both MaSp1 and MaSp2 NTD fold into 5  $\alpha$ -helical elements connected by flexible loops.<sup>62,63,65</sup> The dimerization of the NTD in response to changes in pH and ionic conditions is facilitated by an array of electrostatic interactions,<sup>62,64,66</sup> where several conserved acidic residues (D40, E79, E84, and E119) are thought to play critical roles.<sup>64,66,67</sup> Overall, dragline spidroin NTD dimerization in response to changes in pH is a particularly complex and tightly regulated phenomenon, which has been explored through a wide range of experimental techniques, including biochemical and structural investigations<sup>58,62–64,66–70</sup> as well as computational studies.<sup>71–73</sup>

On the other hand, the CTD forms a stable dimer at neutral pH, which in the case of MaSp1 and MaSp2 is tethered via disulfide bonding. At low pH values ( $\sim$ pH 5), on the other hand, there is evidence for structural unfolding, which is likely linked to a protonation event that disrupts a conserved salt bridge interaction.<sup>53,59,74,75</sup> A recombinant ADF4 construct with truncated C-terminus was shown to form aggregates when expressed in insect cells, indicating an essential role of CTD in controlling fiber formation.<sup>76</sup> Previous studies have shown the CTD forms amyloid-like fibrils<sup>53</sup> or molten globule conformations<sup>74</sup> at pH 5 or below and suggest that the CTD might function as a nucleating agent for the formation  $\beta$ -sheets within the repeat domains. In addition, MaSp2 CTD in solution was shown to undergo demixing to form liquid-like droplets when exposed to potassium phosphate at pH 5.5 and below.<sup>55</sup> The molecular mechanism for the transformation of CTD from a folded to unfolded state, including which key residues are involved, is still unclear. Furthermore, the underlying details of how changes in CTD structure might trigger the  $\beta$ -sheet formation in the rest of the protein remains elusive.

The exceptional strength of spider dragline silk fiber arises from  $\beta$ -sheet nanocrystals which are made up mostly from the polyalanine stretches in the MaSp repetitive sequences.<sup>77,78</sup> In the amorphous region, MaSp1 with its GGX motif forms

disordered PPII helix ( $3_1$  helix) structure,<sup>79–81</sup> while MaSp2 with its GPGXX motif adopts elastin-like type II  $\beta$ -turn conformations.<sup>27</sup>

Prior to spinning, the repetitive regions that comprise the majority of the dragline spidroin sequences are largely found in a dynamically disordered state, as seen by probing the native major ampullate gland material,<sup>82,83</sup> while others have also detected the presence of helical structures, particularly PPII helices and  $\alpha$ -helices (the latter possibly contributed by the terminal domains).<sup>52,84</sup> Using recombinant repetitive domain constructs, the occurrence of random-coil and PPII helix conformations was also confirmed.<sup>85</sup> The PPII helix conformation was proposed as the prefibrillar state of the glycine-rich region in solution since this conformation has the capability to undergo intramolecular interactions in response to shear forces and dehydration by forming a reverse turn.<sup>85,86</sup> This finding is also supported by in situ observations in the intact major ampullate glands using vibrational circular dichroism.<sup>84,87</sup>

Unlike the terminal domains, the conformation of the isolated repetitive domain in solution appears to be relatively insensitive to pH changes,<sup>85</sup> although in contrast the conformation and dynamics are significantly affected by the ion composition.<sup>88</sup> Chaotropic ions ( $\text{Na}^+$ ,  $\text{Mg}^{2+}$ ,  $\text{Cl}^-$ ) prevent intra- and intermolecular interactions, particularly in the glycine-rich region, which is required to maintain the solubility of spidroin. On the other hand, the increase in kosmotropic ion concentration in the native spinning ducts promotes hydrogen bonding in the glycine-rich regions, facilitating interactions among polyalanine regions, thereby promoting  $\beta$ -sheet formation.<sup>88</sup> In addition, recent findings showed that the GAA and AAG motifs flanking the polyalanine runs may also be important for silk protein preassembly stabilization.<sup>89</sup>

#### 4. PARADIGMS FOR SPIDER SILK FIBER SELF-ASSEMBLY

We discuss briefly three hypotheses relating to the structural organization of soluble silk proteins in the liquid feedstock and the possible mechanisms for self-assembly into ordered hierarchical fibers (Figure 3). It should be emphasized that these hypotheses are not meant to be mutually exclusive; rather, they represent different paradigms or frameworks that may help make sense of the vast and sometimes seemingly contradictory data that have been collected through various means. Importantly for our purposes here, they might serve as guides for designing biomimetic spinning systems and possibly help to direct future research projects.

**Liquid Crystalline Theory.** Native silk feedstock has unusual flow properties: despite the high viscosity owing to the extremely high protein concentration, the silk dope material readily flows as a liquid within the increasingly narrow tubes of the spinning duct prior to conversion into insoluble fibers with hierarchical organized features extending across multiple length scales. The viscoelastic shear-thinning properties of the silk dope,<sup>90</sup> as observed in rheological experiments, is considered to be key to its spinnability; interestingly, reconstitution of silk dope (that is, denaturation followed by “renaturation” under physiological conditions) leads typically to a loss of the native-like flow properties,<sup>91</sup> suggesting that the behavior of the molecular constituents is governed by precise intermolecular interactions. Such results have led to the formulation of the liquid crystalline (LC) theory for silk assembly<sup>92–94</sup> (Figure 3a), which in essence strives to reconcile observations of

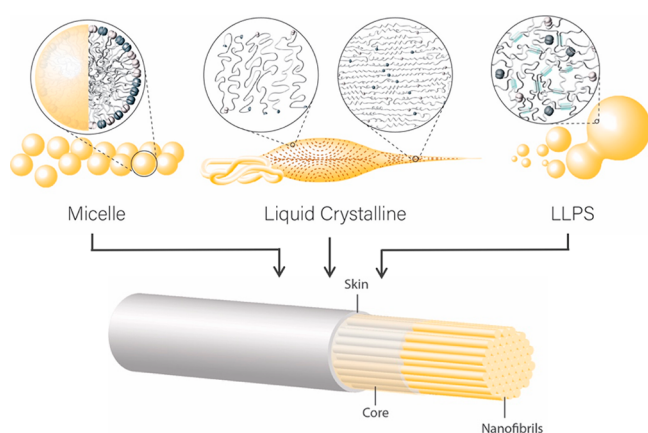


**Figure 3.** Three paradigms for spider silk self-assembly. Arrangement of spidroin chains within the spider silk glands is still largely undetermined. Concentrated protein material must somehow avoid premature aggregation, flow as a liquid inside narrow ducts, and rapidly convert from a disordered state into a hierarchically organized fiber with nanoscale precision, characterized by extreme toughness. Three models are depicted schematically: liquid crystalline (LC), micelle, and liquid–liquid phase separation (LLPS) models.

complex biological phenomena with theories originating from polymer research. A predominant view is that the spidroin chains adopt a compact “string-of-beads” configuration in the soluble state; as the spidroins migrate through the spinning apparatus, changes in the internal geometry of the ducts (with the associated changes in shear stress and extensional flow) combined with the effects of the drawdown steps facilitate a progressive reorientation of the chains, an increase in the number of intermolecular contacts, and the removal of bulk water to produce the native, hierarchically structured silk fiber. The LC framework provides powerful conceptual tools that can inform the design of biomimetic systems for silk spinning<sup>95</sup> with perhaps the greatest applicability to microfluidics systems (see below). On the other hand, from a biochemical perspective, the insights provided by the LC theory are more limited.

**Micelle Theory.** The micelle hypothesis posits that the amphiphilic patterning of amino acid residues along the silk protein sequence leads, in response to an aqueous solvent, to the formation of discrete oligomeric structures (termed micelles), wherein the hydrophobic elements are sequestered within the interior while the more hydrophilic residues are oriented outward where they can interact with the polar environment. The model was first proposed to account for the behavior of fibroin protein constituents of silkworm silk (from *Bombyx mori*), where spherical structures measuring 100–200 nm were observed and which could further assemble into larger assemblies termed globules<sup>96</sup> (Figure 3b). During spinning, the flow and shear forces generated in the narrow ducts are thought to promote a controlled deformation of the globules, leading to the aligned fibrillar structure of silk. The hypothesis has been transposed to the spider silk system, where it has been used to describe the supramolecular arrangement of spidroin molecules in the gland prior to the formation of the insoluble silk fibers.<sup>96</sup> Indeed, there is ample evidence for the occurrence of sphere-like or globular structures within the major ampullate gland storage and spinning apparatus,<sup>56,97</sup> and the presence of aligned granular or spherical nanoscale structures within the interior of dragline silk fiber could be

interpreted to support this view.<sup>97,98</sup> Coarse-grained computational studies have likewise predicted similar assemblies.<sup>99</sup> On the other hand, it is noted that the particular amphiphilic arrangement of residues found in silkworm fibroin is not replicated in spidroin sequences, at least in the case of dragline spidroins.<sup>59</sup> To recap, native MaSp sequence consists of an extended core repetitive region with alternating polyalanine and glycine-rich regions (the latter interspersed with mostly polar residues); this is flanked by the small globular terminal domains: the hydrophilic NTD and the more hydrophobic CTD, the latter forming constitutive dimers. It is not so obvious how such a sequence architecture could adopt the topology of a micelle *sensu stricto*. Among other things, such a model seems to require a very dense packing of the disordered repetitive domains having hydrophobic character within the micelle interior, a good recipe for catastrophic protein aggregation, which is contrary to observations. A recent study<sup>56</sup> sought to clarify the nature of protein assemblies found within the silk dope via NMR and cryo-TEM tomography and demonstrated the presence of discrete, hierarchical nano-assemblies ~300 nm in diameter with an internal structure consisting of flake-like subdomains that is sensitive to shear forces. Continued investigations into supramolecular spidroin assemblies, especially in terms of the ordered arrangement of prefibrillar oligomeric complexes, could yield vital insights into the mechanisms of spider silk self-assembly.<sup>89</sup>

**Liquid–Liquid Phase Separation.** Recent years have seen an explosion of interest in the area of biomolecular condensates, now recognized as a fundamental phenomenon linked to various cellular functions including the formation of membraneless organelles, intracellular signaling, and chromatin organization. In response to triggers such as molecular crowding or partner binding, certain types of proteins can undergo demixing from the aqueous environment and form nonstoichiometric supramolecular assemblies resembling liquid-like droplets through a process of liquid–liquid phase separation (LLPS). The topic also has profound biomedical relevance as the aberrant phase separation behavior and/or toxic deposition of mutated protein variants has been implicated in a number of neurodegenerative disorders, as seen for instance with FUS and TDP43 in amyotrophic lateral sclerosis, huntingtin protein in Huntington’s disease, and tau protein in Alzheimer’s disease.<sup>100,101</sup>

Apart from its involvement in intracellular (mal)functions, LLPS also fulfills essential extracellular roles, for instance, in the controlled deposition of structural proteins, where the process is often referred to as coacervation: it underlies, for example, the formation of elastin networks in the extracellular matrix,<sup>102</sup> as well as the mechanism for squid beak morphogenesis.<sup>103</sup> Biopolymer phase separation is also deployed for *in vivo* structural assembly, as in the secretion of underwater adhesives by the sandcastle worm<sup>48</sup> or in the formation of mussel byssal plaques.<sup>104</sup>

The ability of spidroins to undergo LLPS has been recognized for some time. Exler et al.<sup>105</sup> demonstrated that eADF3 (a recombinant spidroin based on *A. diadematus* ADF3 spidroin consisting of 24 repetitive modules and the CTD) underwent phase separation upon buffer exchange from highly chaotropic conditions into dilute Tris solution with the sample separating into high-density and low-density phases (HDP and LDP, respectively). Addition of potassium phosphate at pH 8 to the HDP allowed it to be drawn into thin fibers, whereas sodium chloride was found to inhibit the phase separation.

Another study found that eADF4(C16), a recombinant spidroin derived from *A. diadematus* ADF4 comprising 16 repetitive modules, could also undergo phase separation upon addition of potassium phosphate at >400 mM to form solidified microspheres with a high  $\beta$ -sheet content.<sup>106</sup> Despite such early observations, LLPS has been relatively underutilized as a paradigm to explore the self-assembly of spider silk.

A recent study<sup>55</sup> explored phase separation of biomimetic MaSp2 constructs in considerable detail. The exposure of MaSp2 to multivalent anions (such as phosphate, sulfate, or citrate), above a threshold concentration and at neutral pH, led to phase separation into microscopic liquid-like droplets that readily coalesced into larger structures exhibiting surface wetting properties. The propensity for LLPS was profoundly dependent on various factors including the concentrations of protein and multivalent anions, temperature, pH, as well as spidroin domain composition. On the latter point, experiments using different domain combinations revealed LLPS to be largely governed via the repetitive sequences and the CTD. In the case of the repeat sequences, a higher number of tandem repeats in the MaSp2 construct correlated with a greater propensity for phase separation, whereas the influence of the CTD on LLPS can partly be attributed to the fact that its inclusion effectively doubles the protein chain length (due to constitutive dimer formation); on the other hand, it was also observed that CTD alone could also undergo LLPS, albeit only at lower pH levels. Crucially, exposure to mild acidification (typically to pH 5) combined with the LLPS conditions caused full-domain MaSp2 (N-Rep<sub>n</sub>-C) to rapidly self-assemble into dense nanofibrillar networks. It was shown that the formation of such networks (and, consequently, the ability to be drawn into hierarchically structured macrofibers) required the presence of the three functional domains on the same polypeptide chain; thus, an equimolar mix of N-Rep<sub>n</sub> and Rep<sub>n</sub>-C failed completely to produce any nanofibrillar structures. Native major ampullate silk gland material was also shown to undergo LLPS under the same conditions as the recombinant MaSp2, although the resulting condensates were comparatively smaller and exhibited a less spherical morphology, suggesting a greater tendency to undergo a liquid-to-solid transition.

Other studies confirm the facility of spidroins for LLPS and from there transition into more solid-like fibrillar structures. A hybrid construct consisting of ADF3 repetitive domains flanked on either end by a cellulose binding module (CBM) from the bacterium *Clostridium thermocellum* was shown to undergo phase separation at high protein concentrations into reversible liquid-like droplets.<sup>107</sup> The addition of potassium phosphate generated more solid-like spherical structures, which could be drawn into thin fibers that exhibited surface adhesion and self-fusing properties, indicating that the fibers retained some dynamic characteristics. A follow-up study explored the influence of different kosmotropic salts on CBM-ADF3-CBM phase separation and analyzed their findings in light of classical nucleation theory for initiation of phase separation.<sup>108</sup>

An analysis of dragline silk protein repetitive sequences shows intriguing parallels with the more established protein sequences associated with LLPS. The emerging consensus is that liquid condensate-forming proteins tend to be structurally disordered (i.e., intrinsically disordered proteins or regions) with sequences that often feature repetitive arrays of amino acid motifs. There is typically a low overall sequence

complexity with an enrichment for residues such as Gly, Ser, Tyr, and Gln, which incidentally resembles the composition of the MaSp1/2 Gly-rich regions. The liquid-like behavior of the condensates has been linked to the multivalent architecture of the protein sequences, which enables the formation of a dense and dynamically shifting network of weak intermolecular interactions, as conceptualized, for instance, in the so-called “stickers-and-spacers” model<sup>109–111</sup> (Figure 3c).

Further investigations into spider silk proteins through the prism of biomolecular condensates, with its theoretical underpinnings and associated experimental approaches, could yield new insights regarding mechanisms of self-assembly and lead to advances in biomimetic methods of fiber spinning.

## 5. BIOMIMETIC STRATEGIES

Spurred by the promise of manufacturing ultra-high-performance biobased fibers, there have been various attempts over the years to create artificial spider silk fibers based on recombinant spidroins. The most widely used methods employ variations on the following: purified recombinant spidroins are solubilized in an organic solvent (typically hexafluoroisopropanol) to produce concentrated silk dope, which is then subjected to fiber spinning. In the case of wet spinning, the liquid dope is extruded through a spinneret into a coagulation bath (e.g., isopropanol) that induces its rapid solidification and then reeled into continuous fibers. This can be combined with postprocessing steps, such as postdrawing or heating, which help to induce the formation of  $\beta$ -sheet cross-links, the main determinant of silk fiber strength. Such conventional methods are advantageous from the standpoint of scalability and importantly can readily circumvent problems associated with solubilization of large, disordered protein chains in aqueous media. A comparison of the mechanical properties that can be achieved through recombinant spidroin spinning under denaturing conditions can be found in recent reviews.<sup>3,112</sup>

In recent years, the concept of “biomimetic spider silk” has steadily gained prominence. The basic idea is that in order to produce artificial spider silk that is “just like the real thing”, it would be necessary to emulate the complexity of the in vivo system as closely as possible, in terms of both the protein components used as well as the processing steps toward silk fiber formation.<sup>5,93,113</sup>

There are several reasons why the development of biomimetic spider silk platforms would be desirable. Firstly, from a purely scientific standpoint, such recombinant platforms would serve as valuable models with which to investigate the biochemistry and structural biology of native spider silks using well-defined sequences and under strictly controlled conditions. This is especially relevant since the native spidroin dope is only found in minute quantities in the silk glands and is moreover highly prone to undergo non-native structural changes or aggregation during extraction. Second, it might be that the extraordinary mechanical properties of native spider silk fiber can only be replicated when the spidroin components encounter the appropriate physiochemical self-assembly triggers. As we have seen, each spidroin domain employs sophisticated mechanisms, dependent on the natively folded protein structure, to ensure the finely tuned sensing of environmental changes and the corresponding conformational changes in the correct spatiotemporal sequence. Such responses are not possible under the denaturing conditions employed in conventional spinning methods and are likely required to achieve the hierarchical structural organization of

the silk fibers across multiple length scales (e.g., the formation of aligned nanofibrillar structures within the fiber). Supporting this view are some recent advances in the mechanical performance of recombinant spider silk fibers produced using only mild biomimetic strategies.<sup>3,112</sup> There is equally the pressing issue of sustainability: across research disciplines, there is a growing realization of the value of transitioning from environmentally harmful manufacturing processes (in the case of silk science, exemplified by a reliance on organic solvents or alcohol treatments during fiber spinning) toward more sustainable or environmentally benign alternatives. If we can manage to make artificial spider silk under benign conditions and with qualities that surpass those achieved under the more conventional techniques, it would be a win–win situation.

Here, a major consideration is the sequence of the recombinant spidroins to be used. Strictly speaking, to be considered biomimetic, a recombinant spidroin construct must contain all three functional domains (NTD, repetitive regions, CTD) with each adopting a native-like fold. An obvious reason for this is that, as discussed previously, each domain fulfills a distinct and essential role during fiber self-assembly (for instance, the precise dimerization pathway of the NTD in response to acidification) without which fiber formation cannot properly occur under native-like conditions. In addition, the terminal domains have been shown to greatly aid in the maintenance of solubility and to counteract the tendency of the extended repetitive regions, largely disordered in solution, to undergo aggregation or fibrillization.<sup>5</sup> Indeed, studies that use recombinant spidroin constructs consisting of repetitive regions and either missing or incomplete terminal domains have noted difficulties in maintaining solubility in aqueous buffers<sup>114,115</sup> or a tendency for premature fiber formation at neutral pH,<sup>116,117</sup> which normally requires acidification. A number of recent studies employed complete or “full-domain” spidroin constructs.<sup>55,118–122</sup> Often, the different domain components are mix-and-matched from different spider species and/or spidroin types, presumably to achieve optimal protein yield or solubility; this is probably a valid strategy provided that the exchanged domains (say, the CTD) function in a similar manner. Regarding the repetitive regions, the use of a larger number of tandem repeats is likely to be advantageous,<sup>55,118,123,124</sup> as this correlates to higher  $\beta$ -sheet composition in the resultant fibers and more native-like mechanical performance, although the manipulation of long repetitive DNA sequences during cloning and the maintenance of solubility in the large recombinant proteins under native conditions can pose major challenges.

It would then be predicted that recombinant spidroins that harbor the full set of domains would behave more similarly to native spidroins under physiological conditions compared to when partial sequences are used. Indeed this is seen, for instance, in the NT2RepCT construct based on *E. australis* MaSp1, which was amenable to concentration to very high levels in aqueous buffer at pH 8 (>500 mg/mL) without undergoing aggregation and displayed native-like viscoelastic rheological properties, characteristics not usually shared by partial constructs.<sup>95,119</sup> The importance of full domain inclusion is also well demonstrated in a study based on recombinant *T. clavipes* MaSp1, where atomic force microscopy showed the assembly of uniform fibril-like nanostructures as prefibrillar structures in the case of full-domain N16C protein, which were not observed in samples with only partial domain composition and which correlate with differences in

the secondary structure, microfibrillar arrangement, and mechanical properties in the corresponding spun fibers.<sup>122</sup>

Our group recently published a study aimed to establish a biomimetic system based on MaSp2 from *T. clavipes*.<sup>55</sup> The results showed how each domain plays distinct roles in response to external cues (NTD, pH responsiveness; repetitive regions and CTD, phosphate-triggered LLPS) and, crucially, how the different domains cooperate in the full-domain constructs to enable rapid self-assembly into hierarchical structures. In this way, full-domain N-R12-C MaSp2 in solution, when subjected to a combination of phase separation, mild acidification, and pultrusion,<sup>125</sup> could readily be converted into macroscopic fibers with a hierarchical architecture consisting of bundled nanofibrils oriented along the longitudinal axis and with the emergence of  $\beta$ -sheet conformations induced by the application of mechanical stress on the nascent fibers.

In terms of methods for spinning recombinant dragline spidroins into continuous fibers, the Scheibel group developed a partially biomimetic system whereby a liquid feedstock consisting of the protein solubilized in aqueous buffer is subjected to wet spinning under denaturing conditions. The recombinant spidroins are usually purified under denaturing conditions, subjected to renaturation under more physiological conditions (using either the “classical” or the “biomimetic” spinning dope regimes) and then extruded in an isopropanol/water bath and reeled into continuous fibers. Using chimeric constructs based on ADF3, Heidebrecht et al.<sup>126</sup> showed that full-domain constructs (12 or 24 tandem repeats flanked by NTD and CTD) treated this way and subjected to poststretching could yield homogeneous fibers with high extensibility with toughness values that approximate that of native dragline fiber. A similar approach was used for a chimeric construct based on the short MaSp1s sequence from *Cyrtophora moluccensis*, which yielded fibers having comparable properties, despite the low molecular weight of the constituent protein.<sup>127</sup>

On the other hand, a more rigorous system (from the viewpoint of biomimicry) was presented by Andersson et al.,<sup>119</sup> who used constructs based on *E. australis* MaSp1 consisting of two repeats flanked by the NTD and CTD (NT2RepCT). Highly concentrated protein solution in aqueous buffer could be processed into continuous fibers by extrusion into an aqueous acidic bath (e.g., 0.5 M sodium acetate buffer, pH 5, 200 mM NaCl). FTIR experiments showed a transition from disordered and  $\alpha$ -helical conformations in the soluble state into structures with high  $\beta$ -sheet abundance (estimated at 60%) upon fiber formation. Interestingly, the  $\beta$ -sheet content of the fibers appeared to vary relative to humidity, which was thought to reflect a low level of fiber crystallinity, as a consequence of the short length of the repeat domain.<sup>128</sup> A recent report showed that the system is compatible with high-throughput production, yielding fibers with reproducible toughness values of  $\sim 74$  MJ/m<sup>3</sup>.<sup>129</sup>

Another interesting development is the application of the method termed straining flow spinning (SFS) toward biomimetic silk assembly. SFS involves a coaxial flow system whereby silk dope and a focusing fluid are induced to flow at different rates before encountering a collection bath where final fiber solidification takes place.<sup>130</sup> In this way, different physiochemical parameters could, at least theoretically, be fine tuned, such as pH, ions, and shear forces, in order to more



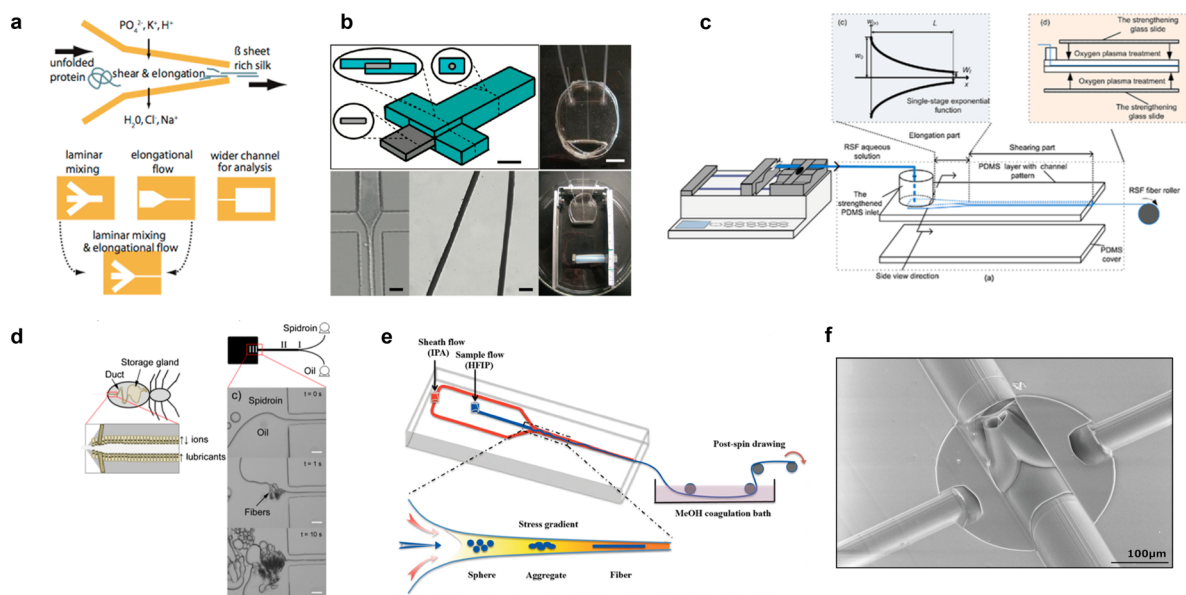


**Figure 4.** Microfluidic designs for silk spinning. Microfluidic devices can provide multiple fluid inlets and customized geometries that can mimic the natural spider silk spinning system. Shown are some examples. (a) Design that incorporates laminar mixing and elongational flow, used to produce recombinant ADF3 fibers by coupling pH gradient, salting out, and elongational flow. (b) Design featuring a multilayer layout with three inlets that can induce hydrodynamic focusing of regenerated silk fibroin material. (c) Device designed to mimic the native shear and elongation conditions of silk glands, allowing direct dry spinning of regenerated silk fibroin. (d) Design with dual laminar flow of recombinant spidroin solution and oil that could produce fibers at the interface. (e) Device with two inlets used to generate fibers from recombinant TuSp1 (eggcase spidroin), upstream of an alcohol coagulation bath. (f) 3D-geometry structure designed using the DLW technique, enabling side-by-side extrusion of dual silk fibers. Panel a reprinted with permission from ref 57. Copyright 2008 National Academy of Sciences, U.S.A. Panel b reprinted with permission from ref 136. Copyright 2011 American Chemical Society. Panel c reprinted with permission from ref 138. Copyright 2014 Elsevier. Panel d reprinted with permission from ref 137. Copyright 2014 Elsevier. Panel e reprinted with permission from ref 140. Copyright 2018 American Chemical Society. Panel f reprinted with permission from ref 142. Copyright 2021 John Wiley and Sons Ltd.

closely replicate the gradual changes found in the natural silk spinning system. Using such a system, NT2RepCT was subjected to 26 different spinning conditions, producing fibers exhibiting a wide range of mechanical properties, demonstrating the crucial importance of spinning parameters.<sup>131</sup>

#### Microfluidics: Current Trends and Next Challenges.

Among the emerging techniques for artificial spider silk assembly, microfluidics promises to provide the closest equivalent to biomimetic conditions: the laminar flow can be designed to precisely control the ionic and pH gradient along the channel, while the elongation flow can be modulated by changing the channel width (Figure 4). Conceptually, what sets microfluidic methods apart from other silk spinning methods is the potential for fine control of the shear forces experienced by the silk protein chains in the narrow channels, which is well known to play a pivotal role in native silk fiber assembly and particularly on the formation of nanocrystalline structures responsible for imparting high tensile strength. Here, however, questions remain regarding the critical shear values necessary for native silk assembly, considerations that are of vital importance in the development of biomimetic microfluidic spinning devices. Although several studies have reported estimates of the shear values, the results have varied widely, perhaps reflecting the different boundary conditions employed in the computational approaches. For silkworm silk gland, the critical shear rate was modeled at around  $1\text{--}10\text{ s}^{-1}$ ,<sup>132,133</sup> while for the spider gland much higher values were predicted, e.g.,  $1500$ <sup>134</sup> and  $2500\text{ s}^{-1}$ .<sup>135</sup> Below, we discuss a number of studies that have used microfluidics techniques toward silk fiber spinning, demonstrating the wide variety of possible approaches.

In a pioneering study, recombinant dragline silk proteins eADF3 and eADF4 were prepared for observation and identification of essential parameters involved in the natural silk assembly.<sup>57</sup> In addition to the flexible regulation of ionic and pH conditions inside the channels, a microfluidic chip could be also designed with various modules to mimic the shear and elongation flow (Figure 4a).

A microfluidics device with a tiered internal design was presented that prevents silk dope from adhering to the walls and maximizes the interface between solutions (Figure 4b). Through the combination of modeling and experiment, it became feasible to predict and tune the properties (such as the Young's modulus and diameter) of the final fibers made from regenerated silk fibroin (RSF) and provides a promising platform to investigate the sequence–structure–property relationship for better mimicking the natural silks.<sup>136</sup>

In the spider spinning apparatus, secreted lubricants presumably help to ensure the smooth flow of silk dope during fiber assembly. Inspired by this, a microfluidics setup that features the laminar flow of an oil-based mobile phase in parallel with silk dope was presented (Figure 4d). Recombinant spidroin solution and the oil were injected into the microfluidic chip via separate channels using positive pressure, allowing the formation of silk fibers within microseconds.<sup>137</sup>

A microfluidic channel with a geometry based on a single-stage exponential function, mimicking the shear and elongation found in natural systems, was designed with the aim of obtaining tough silk fibers (Figure 4c). Concentrated RSF at pH 4.8 and with  $0.3\text{ M Ca}^{2+}$  was injected into the microchip, allowing the fibers to be directly pulled out from the outlet and then reeling in air. Like in native spinning, the fiber could be

dehydrated in air without using a coagulation bath for solidification.<sup>138</sup> Using recombinant MaSp1 repetitive domains, a similar microfluidic device was used upstream of a 70% ethanol coagulation bath followed by continuous postspin drawing on air to produce continuous fibers with a tensile strength of  $286.2 \pm 137.7$  MPa.<sup>139</sup> More recently, the same group used a similar device for microfluidic wet spinning in 90% ethanol at pH 7.4 or 5.0 followed by poststretching in 80% ethanol to generate fibers from recombinant MaSp1 including full-domain constructs. Interestingly, the results show the fibers having a microfibrillar structure and secondary structure and mechanical properties that correlate with the protein domain composition.<sup>122</sup>

Another microfluidic wet-spinning system was recently reported, where spinning dopes composed of combinations of ADF3 and ADF4 were pumped simultaneously with two streams of 30 mM phosphate buffer, pH 8, into a coagulation consisting of 0.5–1 M potassium phosphate buffer at pH 6 followed by alcohol-based poststretching and post-treatment.<sup>121</sup>

A different system with a core–sheath flow design was reported that used recombinant eggcase silk protein dissolved in HFIP as the spinning dope and alcoholic solvent to trigger phase separation. The method could generate different structures ranging from spheres to fibers by modulating the protein concentration and relative flow rate ratio of the microfluidic fluids (Figure 4e).<sup>140</sup>

Another study sought to optimize the performance of microfluidics devices for silk fiber formation and proposed a model having a coaxial structure to generate shear rates up to  $473 \text{ s}^{-1}$ . The fiber diameter could be predicted computationally based on the function of flow rates and the shear force, and the device was used experimentally to produce fibers with 3% PEG as the dehydration agent. It is interesting to find that the shear stress generated by the chip was still several orders of magnitude lower than that in the silkworm gland, which may be one significant reason for the low crystallization in most artificial silk fibers.<sup>141</sup>

In addition, a recent study describes a technique called in-chip direct laser writing (DLW), which marks an advance over conventional methods to achieve coaxial flow (mainly done through manual integration of a glass capillary to a PDMS channel), and has been used to manufacture various designs of spinnerets within the channel, an example of which is shown in Figure 4f.<sup>142</sup>

As illustrated here, considerable progress has been achieved in recent years regarding the development of microfluidics approaches to the production of biomimetic silk fibers. However, there are still major challenges to be made, such as (a) how to replicate the design of in vivo spinning systems, including the fabrication long, narrow microfluidic channels with a circular cross section that would allow the silk protein dope to flow and gradually complete the phase separation without aggregation, (b) how to design the microfluidic chip such that the various chemical triggers are introduced in the correct spatiotemporal order, and (c) how to integrate the different stages of the process to enable the continuous production of biomimetic fibers over extended times, etc.

## 6. CONCLUSION

As recent reports suggest and as we hope this review illustrates, we are still far from having a complete grasp of the true complexity of spider dragline silk. Future studies should

continue to shed light on the details concerning the interactions among the different biomolecular components of spider silk and in doing so allow scientists to better mimic the unique properties of the natural fiber using artificial methods. Such developments would pave the way for the creation of new and exciting materials with high-performance capabilities while minimizing the negative environmental impact.

## AUTHOR INFORMATION

### Corresponding Author

**Keiji Numata** – Biomacromolecules Research Team, Center for Sustainable Resource Science, RIKEN, Wako, Saitama 351-0198, Japan; Department of Material Chemistry, Kyoto University, Kyoto 615-8510, Japan; [orcid.org/0000-0003-2199-7420](https://orcid.org/0000-0003-2199-7420); Email: [keiji.numata@riken.jp](mailto:keiji.numata@riken.jp)

### Authors

**Ali D. Malay** – Biomacromolecules Research Team, Center for Sustainable Resource Science, RIKEN, Wako, Saitama 351-0198, Japan

**Hamish C. Craig** – Biomacromolecules Research Team, Center for Sustainable Resource Science, RIKEN, Wako, Saitama 351-0198, Japan; [orcid.org/0000-0003-3763-8721](https://orcid.org/0000-0003-3763-8721)

**Jianming Chen** – Biomacromolecules Research Team, Center for Sustainable Resource Science, RIKEN, Wako, Saitama 351-0198, Japan

**Nur Alia Oktaviani** – Biomacromolecules Research Team, Center for Sustainable Resource Science, RIKEN, Wako, Saitama 351-0198, Japan

Complete contact information is available at: <https://pubs.acs.org/10.1021/acs.biomac.1c01682>

### Author Contributions

The manuscript was written through contributions of all authors. All authors have given approval to the final version of the manuscript.

### Notes

The authors declare no competing financial interest.

## ACKNOWLEDGMENTS

This work was supported by grants from the ImPACT Program of Council for Science, Technology and Innovation (Cabinet Office, Government of Japan), by JST ERATO grant number JPMJER1602, Grant-in-Aid for Transformative Research Areas (B), and Material DX to K.N.

## REFERENCES

- (1) Greco, G.; Mastellari, V.; Holland, C.; Pugno, N. M. Comparing modern and classical perspectives on spider silks and webs. *Perspectives on Science* **2021**, *29* (2), 133–156.
- (2) Humenik, M.; Scheibel, T.; Smith, A. Spider silk: understanding the structure–function relationship of a natural fiber. *Prog. Mol. Biol. Transl. Sci.* **2011**, *103*, 131–185.
- (3) Koeppel, A.; Holland, C. Progress and trends in artificial review silk spinning: A systematic review. *ACS Biomater. Sci. Eng.* **2017**, *3* (3), 226–237.
- (4) Lefèvre, T.; Auger, M. Spider silk as a blueprint for greener materials: A review. *Int. Mater. Rev.* **2016**, *61* (2), 127–153.
- (5) Rising, A.; Johansson, J. Toward spinning artificial spider silk. *Nat. Chem. Biol.* **2015**, *11* (5), 309–15.
- (6) Gatesy, J.; Hayashi, C.; Motriuk, D.; Woods, J.; Lewis, R. Extreme diversity, conservation, and convergence of spider silk fibroin sequences. *Science* **2001**, *291* (5513), 2603–2605.

- (7) Hayashi, C. Y.; Shipley, N. H.; Lewis, R. V. Hypotheses that correlate the sequence, structure, and mechanical properties of spider silk proteins. *Int. J. Biol. Macromol.* **1999**, *24* (2–3), 271–275.
- (8) Malay, A. D.; Arakawa, K.; Numata, K. Analysis of repetitive amino acid motifs reveals the essential features of spider dragline silk proteins. *PLoS One* **2017**, *12* (8), No. e0183397.
- (9) Blackledge, T. A.; Pérez-Rigueiro, J.; Plaza, G. R.; Perea, B.; Navarro, A.; Guinea, G. V.; Elices, M. Sequential origin in the high performance properties of orb spider dragline silk. *Sci. Rep.* **2012**, *2* (1), 782.
- (10) Blamires, S. J.; Nobbs, M.; Martens, P. J.; Tso, I. M.; Chuang, W.-T.; Chang, C.-K.; Sheu, H.-S. Multiscale mechanisms of nutritionally induced property variation in spider silks. *PLoS One* **2018**, *13* (2), No. e0192005.
- (11) Brooks, A. E.; Steinkraus, H. B.; Nelson, S. R.; Lewis, R. V. An investigation of the divergence of major ampullate silk fibers from *Nephila clavipes* and *Argiope aurantia*. *Biomacromolecules* **2005**, *6* (6), 3095–3099.
- (12) Guehrs, K. H.; Schlott, B.; Grosse, F.; Weisshart, K. Environmental conditions impinge on dragline silk protein composition. *Insect Mol. Biol.* **2008**, *17* (5), 553–564.
- (13) Sanggaard, K. W.; Bechsgaard, J. S.; Fang, X.; Duan, J.; Dyrland, T. F.; Gupta, V.; Jiang, X.; Cheng, L.; Fan, D.; Feng, Y.; et al. Spider genomes provide insight into composition and evolution of venom and silk. *Nat. Commun.* **2014**, *5* (1), 3765.
- (14) Babb, P. L.; Lahens, N. F.; Correa-Garhwal, S. M.; Nicholson, D. N.; Kim, E. J.; Hogenesch, J. B.; Kuntner, M.; Higgins, L.; Hayashi, C. Y.; Agnarsson, I.; Voight, B. F. The *Nephila clavipes* genome highlights the diversity of spider silk genes and their complex expression. *Nat. Genet.* **2017**, *49* (6), 895–903.
- (15) Chaw, R. C.; Correa-Garhwal, S. M.; Clarke, T. H.; Ayoub, N. A.; Hayashi, C. Y. Proteomic evidence for components of spider silk synthesis from black widow silk glands and fibers. *J. Proteome Res.* **2015**, *14* (10), 4223–4231.
- (16) Collin, M. A.; Clarke, T. H., III; Ayoub, N. A.; Hayashi, C. Y. Genomic perspectives of spider silk genes through target capture sequencing: Conservation of stabilization mechanisms and homology-based structural models of spidroin terminal regions. *Int. J. Biol. Macromol.* **2018**, *113*, 829–840.
- (17) Garb, J. E.; Haney, R. A.; Schwager, E. E.; Gregorič, M.; Kuntner, M.; Agnarsson, I.; Blackledge, T. A. The transcriptome of Darwin's bark spider silk glands predicts proteins contributing to dragline silk toughness. *Commun. Biol.* **2019**, *2* (1), 275.
- (18) Kono, N.; Nakamura, H.; Mori, M.; Yoshida, Y.; Ohtoshi, R.; Malay, A. D.; Pedrazzoli Moran, D. A.; Tomita, M.; Numata, K.; Arakawa, K. Multicomponent nature underlies the extraordinary mechanical properties of spider dragline silk. *Proc. Natl. Acad. Sci. U. S. A.* **2021**, *118* (31), No. e2107065118.
- (19) Kono, N.; Nakamura, H.; Ohtoshi, R.; Moran, D. A. P.; Shinohara, A.; Yoshida, Y.; Fujiwara, M.; Mori, M.; Tomita, M.; Arakawa, K. Orb-weaving spider *Araneus ventricosus* genome elucidates the spidroin gene catalogue. *Sci. Rep.* **2019**, *9* (1), 8380.
- (20) Kono, N.; Ohtoshi, R.; Malay, A. D.; Mori, M.; Masunaga, H.; Yoshida, Y.; Nakamura, H.; Numata, K.; Arakawa, K. Darwin's bark spider shares a spidroin repertoire with *Caerostris extrusa* but achieves extraordinary silk toughness through gene expression. *Open Biol.* **2021**, *11* (12), 210242.
- (21) Agnarsson, I.; Kuntner, M.; Blackledge, T. A. Bioprospecting finds the toughest biological material: extraordinary silk from a giant riverine orb spider. *PLoS One* **2010**, *5* (9), e11234.
- (22) Larracas, C.; Hekman, R.; Dyrness, S.; Arata, A.; Williams, C.; Crawford, T.; Vierra, C. A. Comprehensive proteomic analysis of spider dragline silk from black widows: A recipe to build synthetic silk fibers. *Int. J. Mol. Sci.* **2016**, *17* (9), 1537.
- (23) Scharff, N.; Coddington, J. A.; Blackledge, T. A.; Agnarsson, I.; Framenau, V. W.; Szüts, T.; Hayashi, C. Y.; Dimitrov, D. Phylogeny of the orb-weaving spider family Araneidae (Araneae: Araneoidea). *Cladistics* **2020**, *36* (1), 1–21.
- (24) Liu, Y.; Spöner, A.; Porter, D.; Vollrath, F. Proline and processing of spider silks. *Biomacromolecules* **2008**, *9* (1), 116–121.
- (25) Spöner, A.; Unger, E.; Grosse, F.; Weisshart, K. Differential polymerization of the two main protein components of dragline silk during fibre spinning. *Nat. Mater.* **2005**, *4* (10), 772–5.
- (26) Vollrath, F.; Holtet, T.; Thøgersen, H. C.; Frische, S. Structural organization of spider silk. *Proc. R. Soc. London, Ser. B: Biol. Sci.* **1996**, *263* (1367), 147–151.
- (27) Jenkins, J. E.; Creager, M. S.; Butler, E. B.; Lewis, R. V.; Yarger, J. L.; Holland, G. P. Solid-state NMR evidence for elastin-like  $\beta$ -turn structure in spider dragline silk. *Chem. Commun.* **2010**, *46* (36), 6714–6716.
- (28) Savage, K. N.; Gosline, J. M. The role of proline in the elastic mechanism of hydrated spider silks. *J. Exp. Biol.* **2008**, *211* (12), 1948–1957.
- (29) Greco, G.; Arndt, T.; Schmuck, B.; Francis, J.; Bäcklund, F. G.; Shilkova, O.; Barth, A.; Gonska, N.; Seisenbaeva, G.; Kessler, V.; et al. Tyrosine residues mediate supercontraction in biomimetic spider silk. *Commun. Mater.* **2021**, *2* (1), 43.
- (30) Augsten, K.; Muhlig, P.; Herrmann, C. Glycoproteins and skin-core structure in *Nephila clavipes* spider silk observed by light and electron microscopy. *Scanning* **2000**, *22* (1), 12–15.
- (31) Fujiwara, M.; Kono, N.; Hirayama, A.; Malay, A. D.; Nakamura, H.; Ohtoshi, R.; Numata, K.; Tomita, M.; Arakawa, K. Xanthurenic acid is the main pigment of *Trichonephila clavata* gold dragline silk. *Biomolecules* **2021**, *11* (4), 563.
- (32) Schulz, S. Composition of the silk lipids of the spider *Nephila clavipes*. *Lipids* **2001**, *36* (6), 637–647.
- (33) Spöner, A.; Vater, W.; Monajembashi, S.; Unger, E.; Grosse, F.; Weisshart, K. Composition and hierarchical organisation of a spider silk. *PLoS One* **2007**, *2* (10), e998.
- (34) Yazawa, K.; Malay, A. D.; Masunaga, H.; Numata, K. Role of skin layers on mechanical properties and supercontraction of spider dragline silk fiber. *Macromol. Biosci.* **2019**, *19* (3), 1800220.
- (35) Clarke, T. H.; Garb, J. E.; Haney, R. A.; Chaw, R. C.; Hayashi, C. Y.; Ayoub, N. A. Evolutionary shifts in gene expression decoupled from gene duplication across functionally distinct spider silk glands. *Sci. Rep.* **2017**, *7* (1), 8393.
- (36) Clarke, T. H.; Garb, J. E.; Hayashi, C. Y.; Haney, R. A.; Lancaster, A. K.; Corbett, S.; Ayoub, N. A. Multi-tissue transcriptomics of the black widow spider reveals expansions, co-options, and functional processes of the silk gland gene toolkit. *BMC Genomics* **2014**, *15* (1), 365.
- (37) Pham, T.; Chuang, T.; Lin, A.; Joo, H.; Tsai, J.; Crawford, T.; Zhao, L.; Williams, C.; Hsia, Y.; Vierra, C. Dragline silk: a fiber assembled with low-molecular-weight cysteine-rich proteins. *Biomacromolecules* **2014**, *15* (11), 4073–81.
- (38) Esteves, F. G.; dos Santos-Pinto, J. R. A.; Ferro, M.; Sialana, F. J.; Smidak, R.; Rares, L. C.; Nussbaumer, T.; Rattei, T.; Bilban, M.; Bacci Junior, M.; Lubec, G.; Palma, M. S. Revealing the venomous secrets of the spider's web. *J. Proteome Res.* **2020**, *19* (8), 3044–3059.
- (39) Goldberga, I.; Li, R.; Duer, M. J. Collagen structure–function relationships from solid-state NMR spectroscopy. *Acc. Chem. Res.* **2018**, *51* (7), 1621–1629.
- (40) Whaite, A. D.; Wang, T.; Macdonald, J.; Cummins, S. F. Major ampullate silk gland transcriptomes and fibre proteomes of the golden orb-weavers, *Nephila plumipes* and *Nephila pilipes* (Araneae: Nephilidae). *PLoS One* **2018**, *13* (10), No. e0204243.
- (41) dos Santos-Pinto, J. R. A.; Lamprecht, G.; Chen, W. Q.; Heo, S.; Hardy, J. G.; Prielwalder, H.; Scheibel, T. R.; Palma, M. S.; Lubec, G. Structure and post-translational modifications of the web silk protein spidroin-1 from *Nephila spiders*. *J. Proteomics* **2014**, *105*, 174–185.
- (42) dos Santos-Pinto, J. R. A.; Arcuri, H. A.; Lubec, G.; Palma, M. S. Structural characterization of the major ampullate silk spidroin-2 protein produced by the spider *Nephila clavipes*. *Biochim. Biophys. Acta, Proteins Proteomics* **2016**, *1864* (10), 1444–1454.

- (43) dos Santos-Pinto, J. R. A.; Arcuri, H. A.; Priewalder, H.; Salles, H. C.; Palma, M. S.; Lubec, G. Structural model for the spider silk protein spidroin-1. *J. Proteome Res.* **2015**, *14* (9), 3859–3870.
- (44) Raven, D. J.; Earland, C.; Little, M. Occurrence of dityrosine in Tussah silk fibroin and keratin. *Biochim. Biophys. Acta, Protein Struct.* **1971**, *251* (1), 96–99.
- (45) Partlow, B. P.; Applegate, M. B.; Omenetto, F. G.; Kaplan, D. L. Dityrosine cross-linking in designing biomaterials. *ACS Biomater. Sci. Eng.* **2016**, *2* (12), 2108–2121.
- (46) Jensen, R. A.; Morse, D. E. The bioadhesive of *Phragmatopoma californica* tubes - a silk-like cement containing L-Dopa. *J. Comp. Physiol., B* **1988**, *158* (3), 317–324.
- (47) Partlow, B. P.; Bagheri, M.; Harden, J. L.; Kaplan, D. L. Tyrosine templating in the self-assembly and crystallization of silk fibroin. *Biomacromolecules* **2016**, *17* (11), 3570–3579.
- (48) Stewart, R. J.; Wang, C. S.; Shao, H. Complex coacervates as a foundation for synthetic underwater adhesives. *Adv. Colloid Interface Sci.* **2011**, *167* (1–2), 85–93.
- (49) Jain, D.; Zhang, C.; Cool, L. R.; Blackledge, T. A.; Wesdemiotis, C.; Miyoshi, T.; Dhinojwala, A. Composition and function of spider glues maintained during the evolution of cobwebs. *Biomacromolecules* **2015**, *16* (10), 3373–3380.
- (50) Craig, H. C.; Blamires, S. J.; Sani, M. A.; Kasumovic, M. M.; Rawal, A.; Hook, J. M. DNP NMR spectroscopy reveals new structures, residues and interactions in wild spider silks. *Chem. Commun.* **2019**, *55* (32), 4687–4690.
- (51) dos Santos-Pinto, J. R. A.; Arcuri, H. A.; Esteves, F. G.; Palma, M. S.; Lubec, G. Spider silk proteome provides insight into the structural characterization of *Nephila clavipes* flagelliform spidroin. *Sci. Rep.* **2018**, *8*, 14674.
- (52) Hijirida, D. H.; Do, K. G.; Michal, C.; Wong, S.; Zax, D.; Jelinski, L. W. <sup>13</sup>C NMR of *Nephila clavipes* major ampullate silk gland. *Biophys. J.* **1996**, *71* (6), 3442–3447.
- (53) Andersson, M.; Chen, G.; Otikovs, M.; Landreh, M.; Nordling, K.; Kronqvist, N.; Westermarck, P.; Jörnvall, H.; Knight, S.; Ridderstrale, Y.; Holm, L.; Meng, Q.; Jaudzems, K.; Chesler, M.; Johansson, J.; Rising, A. Carbonic anhydrase generates CO<sub>2</sub> and H<sup>+</sup> that drive spider silk formation via opposite effects in the terminal domains. *PLoS Biol.* **2014**, *12* (8), No. e1001921.
- (54) Knight, D. P.; Vollrath, F. Changes in element composition along the spinning duct in a *Nephila* spider. *Naturwissenschaften* **2001**, *88* (4), 179–182.
- (55) Malay, A. D.; Suzuki, T.; Katashima, T.; Kono, N.; Arakawa, K.; Numata, K. Spider silk self-assembly via modular liquid-liquid phase separation and nanofibrillation. *Sci. Adv.* **2020**, *6* (45), eabb6030.
- (56) Parent, L. R.; Onofrei, D.; Xu, D.; Stengel, D.; Roehling, J. D.; Addison, J. B.; Forman, C.; Amin, S. A.; Cherry, B. R.; Yarger, J. L.; et al. Hierarchical spidroin micellar nanoparticles as the fundamental precursors of spider silks. *Proc. Natl. Acad. Sci. U. S. A.* **2018**, *115* (45), 11507–11512.
- (57) Rammensee, S.; Slotta, U.; Scheibel, T.; Bausch, A. R. Assembly mechanism of recombinant spider silk proteins. *Proc. Natl. Acad. Sci. U. S. A.* **2008**, *105* (18), 6590–5.
- (58) Askarieh, G.; Hedhammar, M.; Nordling, K.; Saenz, A.; Casals, C.; Rising, A.; Johansson, J.; Knight, S. D. Self-assembly of spider silk proteins is controlled by a pH-sensitive relay. *Nature* **2010**, *465* (7295), 236–8.
- (59) Hagn, F.; Eisoldt, L.; Hardy, J. G.; Vendrely, C.; Coles, M.; Scheibel, T.; Kessler, H. A conserved spider silk domain acts as a molecular switch that controls fibre assembly. *Nature* **2010**, *465* (7295), 239–42.
- (60) Challis, R. J.; Goodacre, S. L.; Hewitt, G. M. Evolution of spider silks: conservation and diversification of the C-terminus. *Insect Mol. Biol.* **2006**, *15* (1), 45–56.
- (61) Motriuk-Smith, D.; Smith, A.; Hayashi, C. Y.; Lewis, R. V. Analysis of the conserved N-terminal domains in major ampullate spider silk proteins. *Biomacromolecules* **2005**, *6* (6), 3152–3159.
- (62) Hagn, F.; Thamm, C.; Scheibel, T.; Kessler, H. pH-dependent dimerization and salt-dependent stabilization of the N-terminal domain of spider dragline silk—implications for fiber formation. *Angew. Chem., Int. Ed. Engl.* **2011**, *50* (1), 310–3.
- (63) Jaudzems, K.; Askarieh, G.; Landreh, M.; Nordling, K.; Hedhammar, M.; Jörnvall, H.; Rising, A.; Knight, S. D.; Johansson, J. pH-dependent dimerization of spider silk N-terminal domain requires relocation of a wedged tryptophan side chain. *J. Mol. Biol.* **2012**, *422* (4), 477–487.
- (64) Kronqvist, N.; Otikovs, M.; Chmyrov, V.; Chen, G.; Andersson, M.; Nordling, K.; Landreh, M.; Sarr, M.; Jörnvall, H.; Wennmalm, S.; et al. Sequential pH-driven dimerization and stabilization of the N-terminal domain enables rapid spider silk formation. *Nat. Commun.* **2014**, *5*, 3254.
- (65) Oktaviani, N. A.; Malay, A. D.; Matsugami, A.; Hayashi, F.; Numata, K. Nearly complete <sup>1</sup>H, <sup>13</sup>C and <sup>15</sup>N chemical shift assignment of monomeric form of N-terminal domain of *Nephila clavipes* major ampullate spidroin 2. *Biomol. NMR Assignments* **2020**, *14* (2), 335–338.
- (66) Bauer, J.; Schaal, D.; Eisoldt, L.; Schweimer, K.; Schwarzinger, S.; Scheibel, T. Acidic residues control the dimerization of the N-terminal domain of black widow spiders' major ampullate spidroin 1. *Sci. Rep.* **2016**, *6* (1), 34442.
- (67) Otikovs, M.; Chen, G.; Nordling, K.; Landreh, M.; Meng, Q.; Jörnvall, H.; Kronqvist, N.; Rising, A.; Johansson, J.; Jaudzems, K. Diversified structural basis of a conserved molecular mechanism for pH-dependent dimerization in spider silk N-terminal domains. *ChemBioChem.* **2015**, *16* (12), 1720–1724.
- (68) Gaines, W. A.; Sehorn, M. G.; Marcotte, W. R., Jr Spidroin N-terminal domain promotes a pH-dependent association of silk proteins during self-assembly. *J. Biol. Chem.* **2010**, *285* (52), 40745–40753.
- (69) Landreh, M.; Askarieh, G.; Nordling, K.; Hedhammar, M.; Rising, A.; Casals, C.; Astorga-Wells, J.; Alvelius, G.; Knight, S. D.; Johansson, J.; et al. A pH-dependent dimer lock in spider silk protein. *J. Mol. Biol.* **2010**, *404* (2), 328–336.
- (70) Schwarze, S.; Zwettler, F. U.; Johnson, C. M.; Neuweiler, H. The N-terminal domains of spider silk proteins assemble ultrafast and protected from charge screening. *Nat. Commun.* **2013**, *4* (1), 2815.
- (71) da Silva, F. L. B.; Pasquali, S.; Derreumaux, P.; Dias, L. G. Electrostatics analysis of the mutational and pH effects of the N-terminal domain self-association of the major ampullate spidroin. *Soft Matter* **2016**, *12* (25), 5600–5612.
- (72) Kurut, A.; Dicko, C.; Lund, M. Dimerization of terminal domains in spiders silk proteins is controlled by electrostatic anisotropy and modulated by hydrophobic patches. *ACS Biomater. Sci. Eng.* **2015**, *1* (6), 363–371.
- (73) Wallace, J. A.; Shen, J. K. Unraveling a trap-and-trigger mechanism in the pH-sensitive self-assembly of spider silk proteins. *J. Phys. Chem. Lett.* **2012**, *3* (5), 658–662.
- (74) Gauthier, M.; Leclerc, J.; Lefèvre, T.; Gagné, S. M.; Auger, M. Effect of pH on the structure of the recombinant C-terminal domain of *Nephila clavipes* dragline silk protein. *Biomacromolecules* **2014**, *15* (12), 4447–4454.
- (75) Strickland, M.; Tudorica, V.; Řezáč, M.; Thomas, N. R.; Goodacre, S. L. Conservation of a pH-sensitive structure in the C-terminal region of spider silk extends across the entire silk gene family. *Heredity* **2018**, *120* (6), 574–580.
- (76) Ittah, S.; Cohen, S.; Garty, S.; Cohn, D.; Gat, U. An essential role for the C-terminal domain of a dragline spider silk protein in directing fiber formation. *Biomacromolecules* **2006**, *7* (6), 1790–1795.
- (77) Ketten, S.; Xu, Z.; Ihle, B.; Buehler, M. J. Nanoconfinement controls stiffness, strength and mechanical toughness of  $\beta$ -sheet crystals in silk. *Nat. Mater.* **2010**, *9* (4), 359–367.
- (78) Simmons, A.; Ray, E.; Jelinski, L. W. Solid-state <sup>13</sup>C NMR of *Nephila clavipes* dragline silk establishes structure and identity of crystalline regions. *Macromolecules* **1994**, *27* (18), 5235–5237.
- (79) Holland, G. P.; Creager, M. S.; Jenkins, J. E.; Lewis, R. V.; Yarger, J. L. Determining secondary structure in spider dragline silk by carbon–carbon correlation solid-state NMR spectroscopy. *J. Am. Chem. Soc.* **2008**, *130* (30), 9871–9877.

- (80) Holland, G. P.; Jenkins, J. E.; Creager, M. S.; Lewis, R. V.; Yarger, J. L. Quantifying the fraction of glycine and alanine in  $\beta$ -sheet and helical conformations in spider dragline silk using solid-state NMR. *Chem. Commun.* **2008**, *43*, 5568.
- (81) van Beek, J. D.; Hess, S.; Vollrath, F.; Meier, B. H. The molecular structure of spider dragline silk: Folding and orientation of the protein backbone. *Proc. Natl. Acad. Sci. U. S. A.* **2002**, *99* (16), 10266–10271.
- (82) Hronska, M.; Van Beek, J. D.; Williamson, P. T. F.; Vollrath, F.; Meier, B. H. NMR characterization of native liquid spider dragline silk from *Nephila edulis*. *Biomacromolecules* **2004**, *5* (3), 834–839.
- (83) Jenkins, J. E.; Holland, G. P.; Yarger, J. L. High resolution magic angle spinning NMR investigation of silk protein structure within major ampullate glands of orb weaving spiders. *Soft Matter* **2012**, *8* (6), 1947–1954.
- (84) Lefèvre, T.; Leclerc, J.; Rioux-Dubé, J.-F.; Buffeteau, T.; Paquin, M.-C.; Rousseau, M.-E.; Cloutier, I.; Auger, M.; Gagné, S. M.; Boudreault, S.; Cloutier, C.; Pérolet, M. Conformation of spider silk proteins *in situ* in the intact major ampullate gland and in solution. *Biomacromolecules* **2007**, *8* (8), 2342–2344.
- (85) Oktaviani, N. A.; Matsugami, A.; Malay, A. D.; Hayashi, F.; Kaplan, D. L.; Numata, K. Conformation and dynamics of soluble repetitive domain elucidates the initial  $\beta$ -sheet formation of spider silk. *Nat. Commun.* **2018**, *9* (1), 2121.
- (86) Adzhubei, A. A.; Sternberg, M. J. E. Conservation of polyproline II helices in homologous proteins: Implications for structure prediction by model building. *Protein Sci.* **1994**, *3* (12), 2395–2410.
- (87) Lefèvre, T.; Boudreault, S.; Cloutier, C.; Pérolet, M. Conformational and orientational transformation of silk proteins in the major ampullate gland of *Nephila clavipes* spiders. *Biomacromolecules* **2008**, *9* (9), 2399–2407.
- (88) Oktaviani, N. A.; Matsugami, A.; Hayashi, F.; Numata, K. Ion effects on the conformation and dynamics of repetitive domains of a spider silk protein: implications for solubility and beta-sheet formation. *Chem. Commun.* **2019**, *55*, 9761–9764.
- (89) Onofrei, D.; Stengel, D.; Jia, D.; Johnson, H. R.; Trescott, S.; Soni, A.; Addison, B.; Muthukumar, M.; Holland, G. P. Investigating the atomic and mesoscale interactions that facilitate spider silk protein pre-assembly. *Biomacromolecules* **2021**, *22* (8), 3377–3385.
- (90) Kojic, N.; Bico, J.; Clasen, C.; McKinley, G. H. *Ex vivo* rheology of spider silk. *J. Exp. Biol.* **2006**, *209* (21), 4355–4362.
- (91) Holland, C.; Terry, A. E.; Porter, D.; Vollrath, F. Natural and unnatural silks. *Polymer* **2007**, *48* (12), 3388–3392.
- (92) Vollrath, F.; Knight, D. P. Liquid crystalline spinning of spider silk. *Nature* **2001**, *410* (6828), 541–8.
- (93) Vollrath, F.; Porter, D. Silks as ancient models for modern polymers. *Polymer* **2009**, *50* (24), 5623–5632.
- (94) Willcox, P. J.; Gido, S. P.; Muller, W.; Kaplan, D. L. Evidence of a cholesteric liquid crystalline phase in natural silk spinning processes. *Macromolecules* **1996**, *29* (15), 5106–5110.
- (95) Arndt, T.; Laity, P. R.; Johansson, J.; Holland, C.; Rising, A. Native-like flow properties of an artificial spider silk dope. *ACS Biomater. Sci. Eng.* **2021**, *7* (2), 462–471.
- (96) Jin, H.-J.; Kaplan, D. L. Mechanism of silk processing in insects and spiders. *Nature* **2003**, *424*, 1057.
- (97) Lin, T. Y.; Masunaga, H.; Sato, R.; Malay, A. D.; Toyooka, K.; Hikima, T.; Numata, K. Liquid crystalline granules align in a hierarchical structure to produce spider dragline microfibrils. *Biomacromolecules* **2017**, *18* (4), 1350–1355.
- (98) Du, N.; Liu, X. Y.; Narayanan, J.; Li, L.; Lim, M. L. M.; Li, D. Design of superior spider silk: From nanostructure to mechanical properties. *Biophys. J.* **2006**, *91* (12), 4528–4535.
- (99) Lin, S.; Ryu, S.; Tokareva, O.; Gronau, G.; Jacobsen, M. M.; Huang, W.; Rizzo, D. J.; Li, D.; Staii, C.; Pugno, N. M.; et al. Predictive modelling-based design and experiments for synthesis and spinning of bioinspired silk fibres. *Nat. Commun.* **2015**, *6* (1), 6892.
- (100) Alberti, S.; Hyman, A. A. Biomolecular condensates at the nexus of cellular stress, protein aggregation disease and ageing. *Nat. Rev. Mol. Cell Biol.* **2021**, *22* (3), 196–213.
- (101) Shin, Y.; Brangwynne, C. P. Liquid phase condensation in cell physiology and disease. *Science* **2017**, *357* (6357), eaaf4382.
- (102) Muiznieks, L. D.; Cirulis, J. T.; van der Horst, A.; Reinhardt, D. P.; Wuite, G. J. L.; Pomès, R.; Keeley, F. W. Modulated growth, stability and interactions of liquid-like coacervate assemblies of elastin. *Matrix Biol.* **2014**, *36*, 39–50.
- (103) Tan, Y.; Hoon, S.; Guerette, P. A.; Wei, W.; Ghadban, A.; Hao, C.; Miserez, A.; Waite, J. H. Infiltration of chitin by protein coacervates defines the squid beak mechanical gradient. *Nat. Chem. Biol.* **2015**, *11* (7), 488–495.
- (104) Astoricchio, E.; Alfano, C.; Rajendran, L.; Temussi, P. A.; Pastore, A. The wide world of coacervates: from the sea to neurodegeneration. *Trends Biochem. Sci.* **2020**, *45* (8), 706–717.
- (105) Exler, J. H.; Hümmerich, D.; Scheibel, T. The amphiphilic properties of spider silks are important for spinning. *Angew. Chem., Int. Ed.* **2007**, *46* (19), 3559–3562.
- (106) Slotta, U. K.; Rammensee, S.; Gorb, S.; Scheibel, T. An engineered spider silk protein forms microspheres. *Angew. Chem., Int. Ed.* **2008**, *47* (24), 4592–4594.
- (107) Mohammadi, P.; Aranko, A. S.; Lemetti, L.; Cenev, Z.; Zhou, Q.; Virtanen, S.; Landowski, C. P.; Penttilä, M.; Fischer, W. J.; Wagermaier, W.; Linder, M. B. Phase transitions as intermediate steps in the formation of molecularly engineered protein fibers. *Commun. Biol.* **2018**, *1*, 86.
- (108) Mohammadi, P.; Jonkergouw, C.; Beaune, G.; Engelhardt, P.; Kamada, A.; Timonen, J. V. I.; Knowles, T. P. J.; Penttilä, M.; Linder, M. B. Controllable coacervation of recombinantly produced spider silk protein using kosmotropic salts. *J. Colloid Interface Sci.* **2020**, *560*, 149–160.
- (109) Banani, S. F.; Lee, H. O.; Hyman, A. A.; Rosen, M. K. Biomolecular condensates: organizers of cellular biochemistry. *Nat. Rev. Mol. Cell Biol.* **2017**, *18* (5), 285–298.
- (110) Dignon, G. L.; Best, R. B.; Mittal, J. Biomolecular phase separation: from molecular driving forces to macroscopic properties. *Annu. Rev. Phys. Chem.* **2020**, *71*, 53–75.
- (111) Martin, E. W.; Holehouse, A. S.; Peran, I.; Farag, M.; Incicco, J. J.; Bremer, A.; Grace, C. R.; Soranno, A.; Pappu, R. V.; Mittag, T. Valence and patterning of aromatic residues determine the phase behavior of prion-like domains. *Science* **2020**, *367* (6478), 694–699.
- (112) Li, J.; Li, S.; Huang, J.; Khan, A. Q.; An, B.; Zhou, X.; Liu, Z.; Zhu, M. Spider silk-inspired artificial fibers. *Adv. Sci.* **2022**, *9* (5), 2103965.
- (113) Vollrath, F.; Porter, D.; Holland, C. There are many more lessons still to be learned from spider silks. *Soft Matter* **2011**, *7* (20), 9595–9600.
- (114) Arcidiacono, S.; Mello, C. M.; Butler, M.; Welsh, E.; Soares, J. W.; Allen, A.; Ziegler, D.; Laue, T.; Chase, S. Aqueous processing and fiber spinning of recombinant spider silks. *Macromolecules* **2002**, *35* (4), 1262–1266.
- (115) Jones, J. A.; Harris, T. I.; Tucker, C. L.; Berg, K. R.; Christy, S. Y.; Day, B. A.; Gaztambide, D. A.; Needham, N. J. C.; Ruben, A. L.; Oliveira, P. F.; et al. More than just fibers: an aqueous method for the production of innovative recombinant spider silk protein materials. *Biomacromolecules* **2015**, *16* (4), 1418–1425.
- (116) Stark, M.; Grip, S.; Rising, A.; Hedhammar, M.; Engström, W.; Hjälml, G.; Johansson, J. Macroscopic fibers self-assembled from recombinant miniature spider silk proteins. *Biomacromolecules* **2007**, *8* (5), 1695–1701.
- (117) Teulé, F.; Furin, W. A.; Cooper, A. R.; Duncan, J. R.; Lewis, R. V. Modifications of spider silk sequences in an attempt to control the mechanical properties of the synthetic fibers. *J. Mater. Sci.* **2007**, *42* (21), 8974–8985.
- (118) Heidebrecht, A.; Eisoldt, L.; Diehl, J.; Schmidt, A.; Geffers, M.; Lang, G.; Scheibel, T. Biomimetic fibers made of recombinant spidroins with the same toughness as natural spider silk. *Adv. Mater.* **2015**, *27* (13), 2189–2194.

- (119) Andersson, M.; Jia, Q.; Abella, A.; Lee, X.-Y.; Landreh, M.; Purhonen, P.; Hebert, H.; Tenje, M.; Robinson, C. V.; Meng, Q.; et al. Biomimetic spinning of artificial spider silk from a chimeric minispidroin. *Nat. Chem. Biol.* **2017**, *13* (3), 262–264.
- (120) Finnigan, W.; Roberts, A. D.; Ligorio, C.; Scrutton, N. S.; Breitling, R.; Blaker, J. J.; Takano, E. The effect of terminal globular domains on the response of recombinant mini-spidroins to fiber spinning triggers. *Sci. Rep.* **2020**, *10* (1), 10671.
- (121) Saric, M.; Eisoldt, L.; Döring, V.; Scheibel, T. Interplay of different major ampullate spidroins during assembly and implications for fiber mechanics. *Adv. Mater.* **2021**, *33* (9), 2006499.
- (122) Hu, C.-F.; Qian, Z.-G.; Peng, Q.; Zhang, Y.; Xia, X.-X. Unconventional spidroin assemblies in aqueous dope for spinning into tough synthetic fibers. *ACS Biomater. Sci. Eng.* **2021**, *7* (8), 3608–3617.
- (123) Xia, X.-X.; Qian, Z.-G.; Ki, C. S.; Park, Y. H.; Kaplan, D. L.; Lee, S. Y. Native-sized recombinant spider silk protein produced in metabolically engineered *Escherichia coli* results in a strong fiber. *Proc. Natl. Acad. Sci. U. S. A.* **2010**, *107*, 14059–14063.
- (124) Bowen, C. H.; Dai, B.; Sargent, C. J.; Bai, W.; Ladiwala, P.; Feng, H.; Huang, W.; Kaplan, D. L.; Galazka, J. M.; Zhang, F. Recombinant spidroins fully replicate primary mechanical properties of natural spider silk. *Biomacromolecules* **2018**, *19* (9), 3853–3860.
- (125) Sparkes, J.; Holland, C. Analysis of the pressure requirements for silk spinning reveals a pultrusion dominated process. *Nat. Commun.* **2017**, *8* (1), 594.
- (126) Heidebrecht, A.; Scheibel, T. Recombinant production of spider silk proteins. *Adv. Appl. Microbiol.* **2013**, *82*, 115–153.
- (127) Thamm, C.; Scheibel, T. Recombinant production, characterization, and fiber spinning of an engineered short major ampullate spidroin (MaSp1s). *Biomacromolecules* **2017**, *18* (4), 1365–1372.
- (128) Otikovs, M.; Andersson, M.; Jia, Q.; Nordling, K.; Meng, Q.; Andreas, L. B.; Pintacuda, G.; Johansson, J.; Rising, A.; Jaudzems, K. Degree of biomimicry of artificial spider silk spinning assessed by NMR spectroscopy. *Angew. Chem., Int. Ed.* **2017**, *129* (41), 12745–12749.
- (129) Schmuck, B.; Greco, G.; Barth, A.; Pugno, N. M.; Johansson, J.; Rising, A. High-yield production of a super-soluble miniature spidroin for biomimetic high-performance materials. *Mater. Today* **2021**, *50*, 16–23.
- (130) Pérez-Rigueiro, J.; Madurga, R.; Gañán-Calvo, A. M.; Plaza, G. R.; Elices, M.; López, P. A.; Daza, R.; González-Nieto, D.; Guinea, G. V. Straining flow spinning of artificial silk fibers: A review. *Biomimetics* **2018**, *3* (4), 29.
- (131) Gonska, N.; López, P. A.; Lozano-Picazo, P.; Thorpe, M.; Guinea, G. V.; Johansson, J.; Barth, A.; Pérez-Rigueiro, J.; Rising, A. Structure–function relationship of artificial spider silk fibers produced by straining flow spinning. *Biomacromolecules* **2020**, *21* (6), 2116–2124.
- (132) Holland, C.; Terry, A. E.; Porter, D.; Vollrath, F. Comparing the rheology of native spider and silkworm spinning dope. *Nat. Mater.* **2006**, *5* (11), 870–874.
- (133) Moriya, M.; Ohgo, K.; Masubuchi, Y.; Asakura, T. Flow analysis of aqueous solution of silk fibroin in the spinneret of *Bombyx mori* silkworm by combination of viscosity measurement and finite element method calculation. *Polymer* **2008**, *49* (4), 952–956.
- (134) Kojic, N.; Kojic, M.; Gudlavalleti, S.; McKinley, G. Solvent removal during synthetic and *Nephila* fiber spinning. *Biomacromolecules* **2004**, *5* (5), 1698–1707.
- (135) Breslauer, D. N.; Lee, L. P.; Muller, S. J. Simulation of flow in the silk gland. *Biomacromolecules* **2009**, *10* (1), 49–57.
- (136) Kinahan, M. E.; Filippidi, E.; Köster, S.; Hu, X.; Evans, H. M.; Pfohl, T.; Kaplan, D. L.; Wong, J. Tunable silk: using microfluidics to fabricate silk fibers with controllable properties. *Biomacromolecules* **2011**, *12* (5), 1504–1511.
- (137) Renberg, B.; Andersson-Svahn, H.; Hedhammar, M. Mimicking silk spinning in a microchip. *Sensors Actuators B: Chem.* **2014**, *195*, 404–408.
- (138) Luo, J.; Zhang, L.; Peng, Q.; Sun, M.; Zhang, Y.; Shao, H.; Hu, X. Tough silk fibers prepared in air using a biomimetic microfluidic chip. *Int. J. Biol. Macromol.* **2014**, *66*, 319–324.
- (139) Peng, Q.; Zhang, Y.; Lu, L.; Shao, H.; Qin, K.; Hu, X.; Xia, X. Recombinant spider silk from aqueous solutions via a bio-inspired microfluidic chip. *Sci. Rep.* **2016**, *6* (1), 35473.
- (140) Chen, J.; Hu, J.; Sasaki, S.; Naka, K. Modular assembly of a conserved repetitive sequence in the spider eggcase silk: From gene to fiber. *ACS Biomater. Sci. Eng.* **2018**, *4*, 2748–2757.
- (141) Li, D.; Jacobsen, M. M.; Gyune Rim, N.; Backman, D.; Kaplan, D. L.; Wong, J. Y. Introducing biomimetic shear and ion gradients to microfluidic spinning improves silk fiber strength. *Biofabrication* **2017**, *9* (2), No. 025025.
- (142) Lügen, A.; Geiger, M.; Steinbeck, L.; Joel, A. C.; Lampert, A.; Linkhorst, J.; Wessling, M. Biocompatible micron-scale silk fibers fabricated by microfluidic wet spinning. *Adv. Healthcare Mater.* **2021**, *10* (20), 2100898.

## Recommended by ACS

### Liquid–Liquid Phase Separation and Assembly of Silk-like Proteins is Dependent on the Polymer Length

Laura Lemetti, A. Sesiija Aranko, *et al.*

JULY 07, 2022  
BIOMACROMOLECULES

READ 

### Mimicking the Natural Basement Membrane for Advanced Tissue Engineering

Puja Jain, Smriti Singh, *et al.*

JULY 15, 2022  
BIOMACROMOLECULES

READ 

### Design of Polypeptides Self-Assembling into Antifouling Coatings: Exploiting Multivalency

Nicolò Alvisi, Renko de Vries, *et al.*

AUGUST 11, 2022  
BIOMACROMOLECULES

READ 

### Nanoarchitected Tough Biological Composites from Assembled Chitinous Scaffolds

Wei Huang, David Kisailus, *et al.*

APRIL 25, 2022  
ACCOUNTS OF CHEMICAL RESEARCH

READ 

Get More Suggestions >